Accepted Manuscript

Synthesis, vasorelaxant activity and 2D-QSAR study of some novel pyridazine derivatives

Riham F. George, Dalia O. Saleh

PII: S0223-5234(15)30397-4

DOI: 10.1016/j.ejmech.2015.12.015

Reference: EJMECH 8255

To appear in: *European Journal of Medicinal Chemistry*

Received Date: 6 October 2015

Revised Date: 8 December 2015

Accepted Date: 9 December 2015

Please cite this article as: R.F. George, D.O. Saleh, Synthesis, vasorelaxant activity and 2D-QSAR study of some novel pyridazine derivatives, *European Journal of Medicinal Chemistry* (2016), doi: 10.1016/j.ejmech.2015.12.015.

Synthesis, vasorelaxant activity and 2D-QSAR study of some novel pyridazine derivatives

Riham F. George [a,*], Dalia O. Saleh[b]

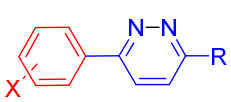

A

X= H, 2-OCH_3, 4-OCH_3, 4-Cl
R= Pyrrolidinyl, imidazolyl, pyrazolyl

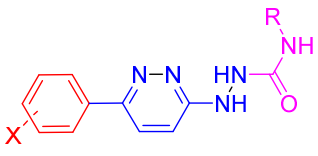

B

X= 2-OCH_3, 4-Cl
R= phenyl, cyclohexyl

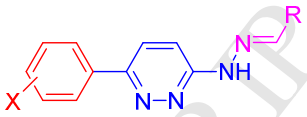

C

X= 2-OCH_3, 4-Cl
R= different aryl

Synthesis, vasorelaxant activity and 2D-QSAR study of some novel pyridazine derivatives

Riham F. George [a,*], Dalia O. Saleh[b]

[a] Pharmaceutical Chemistry department, Faculty of Pharmacy, Cairo University, ElKasr El-Aini street, 11562 Cairo, Egypt
[b] Pharmacology Department, National Research centre, Dokki, Giza 12622, Egypt

Abstract

Novel 3,6-disubstituted pyridazines were synthesized by facile method and screened for their vasorelaxant properties utilizing isolated thoracic rat aortic rings. Compounds **8a** and **11a** exerted potent vasorelaxant activity (IC_{50} = 198 and 177 μM, respectively) relative to doxazosin mesylate (used reference standard, IC_{50} = 226 μM), that, they may represent promising hits for treatment of cardiovascular disorders. The observed activity was validated by a statistically significant QSAR model (N=32, n=6, R^2=0.811782, R^2_{cvOO} = 0.7153, R^2_{cvMO} = 0.7209, F=17.9708, s^2=9.65226x10^{-8}) that was obtained employing CODESSA-Pro software.

Keywords: pyridazines, vasodilator, QSAR

***** Corresponding author. Tel.: +2 01222979898, E-mail address: rihamfgeorge@yahoo.com

1. Introduction

Cardiovascular diseases (CVDs), in particular coronary heart disease and stroke, are the leading cause of mortality in the developed countries. According to the World Health Organization (WHO), 17 million people die every year by CVDs, accounting for almost one third of deaths worldwide per year [1]. Among cardiovascular disorders, hypertension is known as a silent killer as it is the most common risk factor that can cause coronary disease, myocardial infarction, stroke and sudden death. In addition, it is the major contributor to cardiac failure and renal insufficiency [2,3]. Moreover, hypertension is not only responsible for high morbidity and mortality, but it impacts negatively the quality of life of a huge number of people across the world. Therefore, prevention and treatment of hypertension is an important public health challenge. Over the past decades, great efforts have been made to discover many antihypertensive drugs that act through different mechanisms such as: diuretics [4], angiotensin-converting enzyme inhibitors [5,6], angiotensin II receptor blockers [6,7], calcium channel blockers [8], centrally sympathetic α2-adrenoreceptors stimulants [9], and drugs that prevent the action of peripheral sympathetic activity as β-adrenergic [10,11] and α-adrenergic blocking agents [12]. It is noteworthy that the reduction in blood pressure achieved with most of the aforementioned classes of drugs is directly or indirectly related to the relaxation of vascular smooth muscles; which makes vasorelaxation one of important strategies in controlling hypertension [13]. Several agents have been developed; however they are all associated with side effects such as fatigue, mood change, sleep disturbances, etc [14]. Therefore, there is a continuous need to explore and develop new vasorelaxant agents with minimal side effects.

The pyridazine nucleus represents a versatile scaffold to develop new pharmacologically active compounds. This heterocyclic system has a wide range of biological activities and can also be used to link other pharmacophoric groups [15–18]. For instance, the 6-(aryl or heteroaryl)pyridazinone derivatives represent an important core with a wide pharmacological profile that includes interesting activities on cardiovascular system, such as cardiotonic effects [19,20], antihypertensive activity [21] and platelet aggregation inhibition [22]. Zardaverine **I**, levosimendan **II** and motapizone **III** are some characteristic drugs bearing this pharmacophoric moiety [23–25] (Fig. 1).

Most of the described pyridazinone derivatives, showing activity on cardiovascular system, possess aryl residues at position 6 of the pyridazine ring [23,26,27]. Interestingly, 6-hydrazino-3-phenylpyridazine **IV** which exhibited strong hypotensive properties, is the structural analog of the well known vasodilator hydralazine **V** that possesses a phenyl ring attached to the pyridazine nucleous instead of being fused to it as in hydralazine [28] (Figure 1). Encouraged by these findings; this work focused on design and synthesis of some phenylpyridazines substituted with a heterocyclic ring, namely, pyrrolidine, imidazole or pyrazole, (general structure A, Figure 2). These ring systems can be considered as pharmacophoric moieties in many vasorelaxant agents [9,19,21,25,29–31]. Moreover, 6-hydrazino-3-phenylpyridazine **IV** was used for further structural modification through derivatization of the hydrazine moiety into a semicarbazide group (general structure B), or an aryl hydrazone (general structure C, Figure 2) in order to study their effect on the modulation of the activity. Additionally, quantitative structure-activity relationship (QSAR) studies were considered in the present work to validate the obtained vasorelaxant activity and detect the most important structural parameters controlling it.

Figure 1

Figure 2

2- Results and discussion

2.1. Chemistry

The targeted pyridazines were synthesized according to the general procedures outlined in Schemes 1 and 2. Thus, the 6-aryl-3-pyridazinones **3a-d** were synthesized from the reaction of the appropriate acetophenone **1a-d** and glyoxilic acid **2** followed by cyclisation with hydrazine hydrate [32]. Chlorination of **3a-d** with phosphorous oxychloride afforded 3-chloro-6-arylpyridazines **4a-d** which were further treated with hydrazine hydrate in absolute ethanol to obtain the 3-hydrazino derivatives **5a-d** [33]. The target compounds **6a-d** and **7a-c** were obtained from the precursor chloropyridazines **4a-d** through a nucleophilic substitution reaction with imidazole and pyrrolidine, respectively (Scheme 1). The structures of the obtained compounds **6a-d** were confirmed by ^{1}H NMR which revealed three broad singlet signals at 7.30-7.32, 7.81-7.83 and 8.49-

8.53 ppm corresponding to the imidazole protons. Compound **6b** revealed triplet corresponding to the imidazole proton at C2 at 7.83 ppm due to long range coupling with protons at C4, C5 of the imidazole ring. However, the pyridazine protons of **6a-d** appeared as two doublets at 7.59-7.68 and 7.97-8.24 ppm, while the phenyl ring protons of **6a** revealed two multiplets at 7.53-7.59 and 8.10-8.12 ppm. In case of the *p*-substituted derivatives **6b, 6d**, two doublets appeared at the range 7.07-7.56 and 8.07 ppm. On the other hand, the *o*-substituted derivative **6c** showed doublet at 7.08 ppm corresponding to the proton at C3 that coupled with H of C4, two doublet triplets at 7.18 and 7.49 ppm corresponding to protons at C4 and C5 which coupled with protons at C3, C5, C6 and C4, C6, C3, respectively, and one doublet of doublet at 8.04 ppm due to the proton at C6 that coupled with protons at C5 and C4. Moreover, the appearance of multiplet signals in the ranges 2.06-2.12 and a broad singlet at 3.63 ppm corresponding to the pyrrolidine protons attested the obtained compounds **7a,b**. Regarding compound **7c**, the pyrrolidine protons appeared as a multiplet at 1.98-2.01 ppm and a triplet at 3.56 ppm. Meanwhile, cyclocondensation of the hydrazine derivatives **5a-d** with acetyl acetone in absolute ethanol afforded 3-(3,5-dimethyl-1*H*-pyrazol-1-yl)-6-arylpyridazines **8a-d**. ^{1}H NMR spectra of **8c,d** confirmed the obtained structure through the presence of three singlet signals at 2.34, 2.81-2.82 and 3.89-3.90 ppm corresponding to two methyl and one methoxy groups, respectively, in addition to a singlet attributed to the pyrazole proton at 6.08-6.09 ppm. Similarly, the reaction of **5a-d** with either ethoxymethylene malononitrile or ethyl ethoxymethylene cyanoacetate in absolute ethanol gave the 5-aminopyrazole derivatives **9a-d** and **10a-d**, respectively. The IR spectra of **9b-d** and **10 b-d** showed the NH_2 stretching vibration as two bands at 3391-3285 and 3453-3312 cm^{-1}, in addition to the CN band at 2230-2210 cm^{-1} in case of compounds **9b-d**. Moreover, ^{1}H NMR spectra of **10b-d** revealed the triplet-quartet pattern of the C_2H_5 protons at 1.37-1.39 and 4.31-4.34 ppm along with two singlet signals at 7.60-7.62 and 7.82-7.84 ppm corresponding to NH_2 and pyrazole proton, respectively. The former signal for NH_2 was disappeared upon deuteration with D_2O. On the other hand, nucleophilic addition of hydrazines **5a-d** to the appropriate isocyanate in methylene chloride in the presence of triethylamine afforded the semicarbazides **11a-c**, whose structures were confirmed by the appearance of three NH bands at 3329-3300, 3250-3223 and 3138-3134 cm^{-1} in the IR

spectra. In addition, ^{1}H NMR showed three singlet signals corresponding to three NH groups that were exchanged with D_2O. Additionally, the condensation of the hydrazine derivatives **5a-d** with different aromatic aldehydes in absolute ethanol in the presence of catalytic amount of glacial acetic acid revealed the corresponding phenyl hydrazones **12a-h**. These derivatives were characterized by their spectral and elemental data, where ^{1}H NMR spectra revealed the presence of the characteristic singlet signal of methylidene proton at 8.09-8.43 ppm in addition to a singlet signal of NH at 7.84-7.95 or 11.40-11.93 ppm that was disappeared upon treatment with D_2O.

Scheme 1

Scheme 2

2.2. In-vitro vasorelaxant activity

Vasorelaxant properties of the synthesized pyridazines were investigated *in vitro* using isolated thoracic aortic rings of rats precontracted with norepinephrine hydrochloride standard according to the reported procedure [34-40] and compared with doxazosin mesylate as a reference standard. The observed data (Table 1) revealed that all pyridazine derivatives exhibited remarkable vasodilating activity with IC_{50} values ranging from 177–323 μM compared to the reference standard doxazosin mesylate (IC_{50} = 226 μM). It is noteworthy that thirteen compounds (**5a**, **6c**, **8a**, **8b**, **10c**, **10d**, **11a**, **11c**, **12a**, **12c**, **12d**, **12e**, **12h)** showed higher activity than doxazosin mesylate (Table 1). Structure activity relationship (SAR) based on the observed vasorelaxant activity indicated that the impact of the electronic nature of the substituent X viz H, 4-Cl, 2-OCH_3, 4-OCH_3 upon the activity is not absolute. However, substitution with different R resulted in either positive or negative change in the observed activity. Thus, considering the hydrazine derivatives **5a**–**d** as the prototypes of the target compounds, it could be concluded that best results were obtained when the hydrazine group was structurally extended to the semicarbazides **11a**–**c** and hydrazones **12a**–**h**. Moreover, replacement of the hydrazine moiety with rigid azacyclic groups was sometimes in favor of activity as in some imidazolyl **6b,c**, 3,5-dimethylpyrazolyl **8a,b** and 5-amino-4-ethoxycarbonylpyrazolyl derivatives **10b**–**d**. However, with other ring system such as the pyrrolidinyl **7a**–**c** and 5-amino-4-cyanopyrazolyl **9a**–**d**, the activity was diminished.

2.3. 2D- QSAR modeling

2.3.1. Dataset

QSAR is capable of generating a relationship between the chemical structure of an organic compound and its aximu-chemical properties. The vasorelaxant active pyridazines **5a-d**, **6a-d**, **7a,c**, **8a**–**d**, **9a**–**d**, **10a**–**c**, **11a**–**c** and **12a**–**h** were used as a training set in the present QSAR study (homogeneous dataset of common heterocyclic scaffold). The QSAR study was undertaken using comprehensive descriptors for structural and statistical analysis (CODESSA-Pro) software.

2.3.2. Methodology

Geometry of the training set compounds was optimized using the molecular mechanics force field (MM^{+}) followed by the semi-empirical AM1 method implemented in the HyperChem 8.0 package. The structures were fully optimized without fixing any parameters, thus bringing all geometric variables to their equilibrium values. The energy minimization protocol employed the Polak–Ribiere conjugated gradient algorithm. Convergence to a local minimum was achieved when the energy gradient was ≤0.01 kcal mol^{-1}. The RHF (Restricted Hartree-Fock) method was used in spin pairing for the two semi-empirical tools [41–50]. The resulting output files were exported to CODESSA-Pro that includes MOPAC capability for the final geometry optimization.

CODESSA-Pro calculated 725 molecular descriptors including constitutional, topological, geometrical, charge-related, semi-empirical, thermodynamic, molecular-type, atomic-type and bond-type descriptors for the exported 32 bio-active pyridazine-based compounds which were used as training set in the present study. Different mathematical transformations of the experimentally observed vasodilation property/activity (IC_{50}, μM) of the training set compounds were utilized for the QSAR modeling determination including property (IC_{50}, μM), 1/property, log(property) and 1/log(property) values in searching for the best QSAR model.

2.3.3. QSAR modeling

The best multi-linear regression (BMLR) technique was utilized which is a stepwise search for the best n-parameter regression equations (where n stands for the number of descriptors used), based on the highest R^2 (squared correlation coefficient), R^2cvOO (squared cross-validation "leave one-out, LOO" coefficient), R^2cvMO (squared cross-validation "leave many-out, LMO" coefficient), *F* (Fisher statistical significance criteria) values, and s^2 (standard deviation). The QSAR models up to 6 descriptor model describing the bio-activity of the vasorelaxant pyridazine-based active agents were generated (obeying the thumb rule of 5:1, which is the ratio between the data points and the number of QSAR descriptor). The observed and predicted values of the training set compounds **5a–d**, **6a–d**, **7a,c**, **8a–d**, **9a–d**, **10a–c**, **11a–c** and **12a–h** according to the multilinear QSAR models are presented in Table 1.

The statistical characteristics of the BMLR-QSAR model attained are presented in Table 2. The established QSAR model is statistically significant. The descriptors are sorted in the descending order of the respective values of the Student's *t*-criterion, which is a widely accepted measure of statistical significance of individual parameters in multiple linear regressions. Figure 3 shows the QSAR multi-linear model plot of correlations representing the observed *vs.* predicted $1/IC_{50}$ (μM) values for the vasodilation pyridazine-based active agents. The scattered plots are uniformly distributed, covering ranges, observed 0.0031-0.0056, predicted 0.0030-0.0056 log (IC_{50}, μM) units.

Figure 3

2.3.4. Molecular descriptors

Molecular descriptors are the aximu-chemical parameters used to correlate the chemical structure and the bio-property value expressed as $1/IC_{50}$, μM. The descriptors were obtained based on the BMLR method. The first descriptor controlling the attained BMLR-QSAR model based on its level of significance (*t*-criterion = 6.4616) is FHACA fractional HACA (HACA/TMSA) (MOPAC PC) which is a charge-related descriptor.. Fractional hydrogen bonding acceptor ability of the molecule *FHACA1* is determined by equation (1) [51].

$$FHACA1 = \frac{HACA1}{TMSA} \quad \text{..... (1)}$$

Where, HASA1 is the hydrogen bonding acceptor ability, TMSA is the total molecular surface area. The second most important descriptor controlling the BMLR-QSAR model (t = 4.6771) is shadow plane YZ, which is a geometrical descriptor reflecting molecular size. Most geometrical descriptors are calculated directly from the (x,y,z) coordinates and other quantities derived from the coordinates, *e.g.* interatomic distances or distances from a specified origin (*e.g.* the molecule bary-center) [52,53]. The third and fourth descriptors of QSAR model based on their *t*-value (4.1118, -4.9294, respectively) are HA dependent HDSA-1 (Zefirov PC) (all) and HA dependent HDSA-1/TMSA (MOPAC PC) (all), which are a charge-related descriptors. The hydrogen bonding acceptor ability of the molecule HASA1 is determined by equation (2) [51].

$$HASA1 = \sum_A S_A \quad A \in X_{H\text{-}acceptor} \quad \text{..... (2)}$$

Where, S_A stands for solvent-accessible surface area of H-bonding acceptor atoms. The fifth descriptor of the attained QSAR model (t = -5.7082) is structural information content (order 2), which is a topological descriptor determined by equations (3, 4) [51].

$$^{k}SIC = {}^{k}IC / \log_2 n \quad \text{..... (3)}$$

$$^{k}IC = -\sum_{i=1}^{k} \frac{n_i}{n} \log_2 \frac{n_i}{n} \quad \text{..... (4)}$$

Where n_i stands for number of atoms in the i^{th} class, n is the total number of atoms in the molecule, k is the number of atomic layers in the coordination sphere around a given atom that are accounted for. The last descriptor controlling the BMLR-QSAR is 8aximum nucleophilic reaction index for atom C, which is a semi-empirical descriptor. Molecular descriptor values controlling the attained BMLR-QSAR model are presented in Table 3.

2.3.5. Validation of the BMLR-QSAR model

2.3.5.1. Internal validation

Internal validation is applied by the CODESSA-Pro technique employing both leave one out (LOO), which involves developing a number of models with one example omitted at a time, and leave many out (LMO), which involves developing a number of models with many data points omitted at a time (up to 20% of the total data points). The observed

correlations by the internal validation technique are R^2cvOO = 0.715, R^2cvMO = 0.721, respectively which are significantly correlated with the squared correlation coefficient of the attained QSAR model (R^2 = 0.812). Standard deviation of the regression (s^2 = 9.652 x 10^{-8}) is also a measurable value for the attained model together with the Fisher test value (F = 17.971) that reflects the ratio of the variance explained by the model and the variance due to their errors. A high value of the F-test relative to the s2 value is also validation of the model.

The predicted vasodilation properties due to the attained QSAR model of most of the synthesized pyridazines are compatible with their experimentally observed values preserving their relative potencies (Table 1). The predicted IC_{50} value of compound **11a**, which is considered the most potent analogue among all the synthesized pyridazines (IC_{50} = 179 μM) is compatible to its experimentally observed value (IC_{50} = 177 μM) with minor error (error "difference between the observed and predicted values" = -2). The same words for the second most potent pyridazine analogue **8a** (IC_{50} = 198, 210 μM for the observed and predicted values, respectively, error = -12). Compounds **5a**, **6c**, **8b**, **10c**, **11c**, **12a**, **12c** and **12e** which exhibit experimental potency higher than that of doxazosin mesylate (standard reference used), reveal predicted properties correlated with their bio-data (IC_{50} = 206, 205, 213, 225, 207, 209, 217, 205; 214, 213, 216, 232, 198, 215, 219, 201 for the observed and predicted values of **5a**, **6c**, **8b**, **10c**, **11c**, **12a**, **12c** and **12e** μM, respectively). Although high error values due to the observed and predicted vasodilation properties of compounds **12d** and **12h** (which are considered high potent analogue) are slightly high, their bio-properties are still preserved (IC_{50} = 200, 221; 214, 244 μM for the observed and predicted values of **12d** and **12h**, respectively; error = -14, -23 for compounds **12d** and **12h**, respectively). Additionally, correlated predicted bio-data were also revealed due to the QSAR modeling by the promising vasodilation active pyridazines (IC_{50} = 230-323, 226-331 μM for the observed and predicted values) of observed potencies lower than that of doxazosin mesylate.

2.3.5.2. External validation

Compounds **7b** and **10d** were used as an external test set not only for validating the attained QSAR model but also for examining its predicative ability. The test set

analogues experimentally exhibit higher and lower vasodilation potencies relative to the used standard reference (doxazosin mesylate). The variation in potency can indicate the predication capabilities of the attained BMLR-QSAR model. Table 4 reveals the observed and predicted IC_{50} values of the test set compounds. From the observed data, it has been noticed that compound **10d** which is considered a high potent agent (IC_{50} = 216 μM) reveals a predicted IC_{50} = 214 μM with minimum error value = 2. Compounds **7b** that is considered a low potent vasorelaxant active analogue (IC_{50} = 300 μM) afforded predicted IC_{50} = 283 μM (error value = 17).

All the above internal and external validation observations give good sign for the predictive capability of the attained BMLR-QSAR model and support the previous statement concerning its predictive power due to the statistical values.

Table 1. Observed and predicted vasorelaxant activity (IC_{50}, μM) of the training set compounds **5a**–**d**, **6a**–**d**, **7a,c**, **8a**–**d**, **9a**–**d**, **10a**–**c**, **11a**–**c** and **12a**–**h** and doxazosin mesylate.

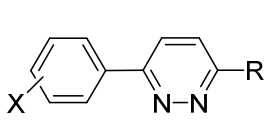

5-9, 7a-c, 10a-d

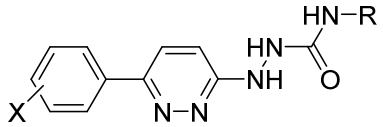

11a-c

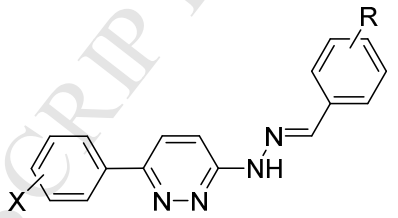

12a-h

Entry	Compd.	R	X	Observed IC_{50}, μM	Predicted IC_{50}, μM	Error
1	**5a**	$NHNH_2$	H	206	214	-8
2	**5b**	$NHNH_2$	4-Cl	275	257	18
3	**5c**	$NHNH_2$	2-OCH_3	279	259	20
4	**5d**	$NHNH_2$	4-OCH_3	235	252	-17
5	**6a**	1-imidazolyl	H	273	256	17
6	**6b**	1-imidazolyl	4-Cl	255	257	-2
7	**6c**	1-imidazolyl	2-OCH_3	205	213	-8
8	**6d**	1-imidazolyl	4-OCH_3	259	269	-10

9	**7a**	1-pyrrolidinyl	H	235	253	-18
10	**7c**	1-pyrrolidinyl	2-OCH_3	284	253	31
11	**8a**	3,5-dimethyl-1*H*-Pyrazol-1-yl	H	198	210	-12
12	**8b**	3,5-dimethyl-1*H*-Pyrazol-1-yl	4-Cl	213	216	-3
13	**8c**	3,5-dimethyl-1*H*-Pyrazol-1-yl	2-OCH_3	299	316	-17
14	**8d**	3,5-dimethyl-1*H*-Pyrazol-1-yl	4-OCH_3	323	315	8
15	**9a**	5-amino-4-cyano-1*H*-pyrazol-1-yl	H	287	291	-4
16	**9b**	5-amino-4-cyano-1*H*-pyrazol-1-yl	4-Cl	310	276	34
17	**9c**	5-amino-4-cyano-1*H*-pyrazol-1-yl	2-OCH_3	316	331	-15
18	**9d**	5-amino-4-cyano-1*H*-pyrazol-1-yl	4-OCH_3	260	235	25
19	**10a**	5-amino-4-ethoxycarbonyl-1*H*-pyrazol-1-yl	H	254	248	6
20	**10b**	5-amino-4-ethoxycarbonyl-1*H*-pyrazol-1-yl	4-Cl	230	268	-38
21	**10c**	5-amino-4-ethoxycarbonyl-1*H*-pyrazol-1-yl	2-OCH_3	225	232	-7
22	**11a**	C_6H_{11}	4-Cl	177	179	-2

23	**11b**	C_6H_{11}	2-OCH_3	266	244	22
24	**11c**	C_6H_5	4-Cl	207	198	9
25	**12a**	4-CF_3	4-Cl	209	215	-6
26	**12b**	4-CF_3	2-OCH_3	248	226	22
27	**12c**	4-OCH_3	4-Cl	217	219	-2
28	**12d**	4-OCH_3	2-OCH_3	200	214	-14
29	**12e**	2,4- $(OCH_3)_2$	4-Cl	205	201	4
30	**12f**	2,4- $(OCH_3)_2$	2-OCH_3	259	230	29
31	**12g**	3,4,5-$(OCH_3)_3$	4-Cl	255	262	-7
32	**12h**	3,4,5-$(OCH_3)_3$	2-OCH_3	221	244	-23
33	**Doxazosin mesylate**	----------	-----	226	----	-----

Table 2. Descriptor of the BMLR-QSAR model for the vasodilatory active pyridazines.

N = 32, n = 6, R^2 = 0.812, R^2cvOO = 0.715, R^2cvMO = 0.721, F = 17.971, s^2 = 9.652 x 10^{-8}					
Entry	ID	Coefficient	*s*	*t*	Descriptor
1	0	0.0096	0.0009	10.1478	Intercept
2	D_1	0.0417	0.0065	6.4616	FHACA Fractional HACA (HACA/TMSA) (MOPAC PC)
3	D_2	5.4842 x 10^{-5}	1.1726 x 10^{-5}	4.6771	Shadow plane YZ
4	D_3	3.3666 x 10^{-5}	8.1877 x 10^{-6}	4.1118	HA dependent HDSA-1 (Zefirov PC) (all)
5	D_4	-0.0245	0.0050	-4.9294	HA dependent HDSA-1/TMSA (MOPAC PC) (all)
6	D_5	-0.0002	3.5491 x 10^{-5}	-5.7082	Structural information content (order 2)
7	D_6	-0.0662	0.0105	-6.2774	Max. nucleoph. React. Index for atom C

$1/IC_{50} = 0.0096 + (0.0417 \times D_1) + [(5.4842 \times 10^{-5}) \times D_2] + [(3.3666 \times 10^{-5}) \times D_3] - (0.0245 \times D_4) - (0.0002 \times D_5) - (0.0662 \times D_6)$

Table 3. Molecular descriptor values of the BMLR-QSAR model for the vasodilatory active pyridazines.

Entry	Compd.	Descriptors*					
		D_1	D_2	D_3	D_4	D_5	D_6
1	**5a**	0.01996	20.8	101.1514	0.22673	19.1222	0.01396
2	**5b**	0.01899	20.42	117.851	0.27135	20.51033	0.01251
3	**5c**	0	32.48	134.0734	0.25586	24.09871	0.01404
4	**5d**	0.02653	20.86	127.3935	0.25483	23.68268	0.0177
5	**6a**	0.01231	21.58	92.5631	0.20305	22.71714	0.01462
6	**6b**	0.01147	21.5	111.6483	0.22665	23.63504	0.01243
7	**6c**	0.01273	33.52	127.8707	0.21346	27.61804	0.01192
8	**6d**	0.01789	21.4	126.9164	0.22294	27.21434	0.0172
9	**7a**	0	31.84	62.98108	0.14203	23.92709	0.01841
10	**7c**	0	38.8	101.1514	0.16894	28.89063	0.01856
11	**8a**	0	35.94	83.97477	0.14995	25.34215	0.01317
12	**8b**	0	31.84	114.5111	0.18407	26.60386	0.01089
13	**8c**	0	36.62	97.33439	0.1944	30.27769	0.01304
14	**8d**	0	30.14	115.4653	0.19416	29.89377	0.01807
15	**9a**	0.02014	27.86	109.7398	0.20324	25.44222	0.03215
16	**9b**	0.02249	28.08	109.7398	0.19697	26.73928	0.02933
17	**9c**	0.02006	35.28	164.6096	0.27947	30.31351	0.02928
18	**9d**	0.02829	28.34	165.5639	0.27831	29.92039	0.01221
19	**10a**	0.03798	33.08	132.1648	0.21973	32.45125	0.02267
20	**10b**	0.03055	32.76	162.224	0.25276	33.66402	0.02149
21	**10c**	0.03443	39.2	176.0607	0.25226	37.26924	0.01691
22	**11a**	0.03008	54.34	107.3541	0.16984	33.74725	0.01374
23	**11b**	0.02384	38.48	134.5505	0.18985	37.48443	0.01397
24	**11c**	0.02546	45.86	91.60884	0.14897	29.75213	0.0236
25	**12a**	0.00534	33.04	74.90931	0.11377	29.853	0.01069
26	**12b**	0.0079	42	153.6357	0.22227	33.79116	0.01112
27	**12c**	0.01256	35.1	127.8707	0.19712	30.91076	0.01098

28	**12d**	0.01251	41.26	129.3021	0.19786	32.49193	0.01013
29	**12e**	0.01348	43.2	167.4724	0.22933	34.16959	0.01059
30	**12f**	0.018	40.9	151.25	0.22414	34.81357	0.01263
31	**12g**	0.01261	41.94	171.7666	0.24847	35.55921	0.01719
32	**12h**	0.01479	46.84	176.0607	0.25802	36.45079	0.01442

* D_1 = FHACA Fractional HACA (HACA/TMSA) (MOPAC PC), D_2 = Shadow plane YZ, D_3 = HA dependent HDSA-1 (Zefirov PC) (all), D_4 = HA dependent HDSA-1/TMSA (MOPAC PC) (all), D_5 = Structural information content (order 2), D_6 = Max. nucleoph. React. Index for atom C.

Table 4. Observed, predicated and molecular descriptor values of external test set compounds **7b** and **10d** according to the BMLR-QSAR model.

Entry	Compd.	Observed IC_{50}, μM	Predicted IC_{50}, μM	Error	Descriptors*					
					D_1	D_2	D_3	D_4	D_5	D_6
1	**7b**	300	283	17	0	25.32	72.52367	0.15211	25.2	0.01664
2	**10d**	216	214	2	0.03495	32.34	178.4464	0.24968	36.89834	0.00912

* D_1 = FHACA Fractional HACA (HACA/TMSA) (MOPAC PC), D_2 = Shadow plane YZ, D_3 = HA dependent HDSA-1 (Zefirov PC) (all), D_4 = HA dependent HDSA-1/TMSA (MOPAC PC) (all), D_5 = Structural information content (order 2), D_6 = Max. nucleoph. React. Index for atom C.

3- Conclusion

In summary, different pyridazines substituted with different aryl/heterocyclic moieties at position 3 and 6 were synthesized by facile methods. All the targeted compounds were screened for their in vitro vasorelaxant activity using isolated thoracic aortic rings of rats precontracted with norepinephrine hydrochloride standard reported procedure and compared with doxazosin mesylate, which was used as a reference standard. All synthesized pyridazine derivatives exhibited remarkable vasodilating activity with IC_{50} values ranges from 177-323 μM compared to the reference standard doxazosin mesylate (IC_{50} = 226 μM). Compounds **8a** and **11a** exerted the highest activity with IC_{50} values 198 and 177 μM, respectively, that, they may represent promising leads for future optimization. 2D-QSAR study was undertaken utilizing CODESSA-Pro software in order to validate the vasorelaxant observed bio-data and determine the most important parameters controlling bio-activity. Statistically significant robust QSAR model describing the pyridazines bio-properties was obtained. External validation technique utilizing high and promising potent synthesized agents, support the predictive power of the attained QSAR model in addition to the internal validation parameters. Homogeneity of the training set analogues (the same chemical scaffold) may be the main factor for the success of the QSAR model.

4. Experimental

4.1. Chemistry

Melting points were recorded on Stuart SMP10 digital melting point apparatus. IR spectra (KBr disc) were recorded on a Shimadzu FT-IR 8400S infrared spectrophotometer. NMR spectra were recorded on a Bruker Ascend 400/ R (^{1}H: 400, ^{13}C: 100 MHz) spectrometer. Some ^{13}C NMR spectra were recorded on a Varian Mercury VX 300 spectrometer (75 MHz). Mass spectra were recorded on a Shimadzu GCMS-QP 1000 EX (EI, 70 eV) spectrometer. Elemental analyses were carried out at the Regional center for Mycology and Biotechnology, Al-Azhar University, Egypt. Compounds **3a**–**d**, **4a**–**d** and **5a**–**d** were prepared according to the reported procedures [32,33].

4.1.1. General procedure for preparation of **6a**–**d** and **7a**–**c**

An equimolar amount of the appropriate secondary amine (2 mmol) and sodium hydride (60% in mineral oil) in dry dimethylformamide (5 ml) was stirred at R.T. for 1 h. The appropriate chloropyridazine derivative **4a**–**d** was added and the mixture was heated at 100˚C for 6 h. The reaction mixture was cooled and poured on ice water. The obtained precipitate was filtered off and washed with water and crystallized from ethanol.

4.1.1.1. 3-(1*H*-Imidazol-1-yl)-6-phenylpyridazine **6a**

Yield 78% (0.43 g), mp 155-157˚C. IR: ν_{max}/ cm^{-1} 3059, 1589, 1562, 1481. ^{1}H NMR ($CDCl_3$, 400 MHz): δ 7.31 (br s, 1H, imidazole proton), 7.53-7.59 (m, 3H, arom. protons), 7.68 (d, 1H, *J*= 9.20 Hz, pyridazine proton), 7.83 (br s, 1H, imidazole proton), 8.04 (d, 1H, *J*= 9.20 Hz, pyridazine proton), 8.10-8.12 (m, 2H, arom. protons), 8.53 (br s, 1H, imidazole proton). ^{13}C NMR ($CDCl_3$, 100 MHz): δ 116.1, 117.4, 126.6, 126.9, 129.2, 130.5, 131.4, 134.9, 135.1, 150.8, 158.5 (arom. carbons). Anal.Calcd. for $C_{13}H_{10}N_4$ (222.25): C, 70.26; H, 4.54; N, 25.21. Found: C, 70.49; H, 4.61; N, 25.42.

4.1.1.2. 3-(4-Chlorophenyl)-6-(1*H*-imidazol-1-yl)pyridazine **6b**

Yield 88% (0.50 g), mp 206-208˚ C. IR: ν_{max}/ cm^{-1} 3042, 1593, 1557, 1489, 1441. ^{1}H NMR (C*D*Cl_3, 400 MHz): δ 7.32 (br s, 1H, imidazole proton), 7.56 (d, 2H, *J*= 8.64 Hz, arom. protons), 7.67 (d, 1H, *J*= 9.20 Hz, pyridazine proton), 7.83 (t, 1H, *J*=1.24 Hz, imidazole proton), 8.02 (d, 1H, *J*= 9.20 Hz, pyridazine proton), 8.07 (d, 2H, *J*= 8.64 Hz, arom. protons), 8.51 (br s, 1H, imidazole proton). ^{13}C NMR (C*D*Cl_3, 75 MHz): δ 115.9, 117.3, 125.8, 126.2, 128.0, 129.4, 131.5, 134.7, 138.4, 158.9, 159.0 (arom. carbons). MS: m/z (%) 256 (M^+, 100), 258 (M^++2, 34). Anal.Calcd. for $C_{13}H_9ClN_4$ (256.69): C, 60.83; H, 3.53; N, 21.83. Found: C, 60.98; H, 3.50; N, 21.98.

4.1.1.3. 3-(1*H*-Imidazol-1-yl)-6-(2-methoxyphenyl)pyridazine **6c**

Yield 80% (0.46 g), mp 159-161˚C. IR: ν_{max}/ cm^{-1} 3050, 2955, 2924, 2853, 1601, 1560, 1491, 1481, 1443. ^{1}H NMR (C*D*Cl_3, 400 MHz): δ 3.92 (s, 3H, OCH_3), 7.08 (d, 1H, *J*= 8.28 Hz, arom. proton), 7.18 (dt, 1H, *J*= 0.74, 7.52, 11.24 Hz, arom.proton), 7.32 (br s, 1H, imidazole proton), 7.49 (dt, 1H, *J*=1.36, 7.86, 10.69 Hz, arom. proton), 7.59 (d, 1H,

J= 9.20 Hz, pyridazine proton), 7.83 (br s, 1H, imidazole proton), 8.04 (dd, 1H, *J*= 1.68, 7.68 Hz, arom. proton), 8.24 (d, 1H, *J*= 9.20 Hz, pyridazine proton), 8.49 (br s, 1H, imidazole proton). MS: m/z (%) 252 (M^+, 34), 253 (M^++1, 7), 185 (100). Anal.Calcd. for $C_{14}H_{12}N_4O$ (252.27): C, 66.65; H, 4.79; N, 22.21. Found: C, 66.98; H, 4.84; N, 22.37.

4.1.1.4. 3-(1*H*-Imidazol-1-yl)-6-(4-methoxyphenyl)pyridazine **6d**

Yield 60% (0.27 g), mp 178-180˚C. IR: ν_{max}/ cm^{-1} 3049-3009, 2965-2837, 1607, 1582, 1508, 1487. ^{1}H NMR (C*D*Cl$_3$, 400 MHz): δ 3.91 (s, 3H, OCH_3), 7.07 (d, 2H, *J*= 8.84 Hz, arom. protons), 7.30 (br s, 1H, imidazole proton), 7.62 (d, 1H, *J*= 9.20 Hz, pyridazine proton), 7.81 (br s, 1H, imidazole proton), 7.97 (d, 1H, *J*= 9.24 Hz, pyridazine proton), 8.07 (d, 2H, *J*= 8.84 Hz, arom. proton), 8.49 (br s, 1H, imidazole proton). ^{13}C NMR (C*D*Cl$_3$, 100 MHz): δ 55.46 (OCH_3), 114.6, 116.0, 117.4, 125.9, 127.6, 128.3, 131.4, 134.8, 150.4, 158.1, 161.65 (arom. carbons). Anal.Calcd. for $C_{14}H_{12}N_4O$ (252.27): C, 66.65; H, 4.79; N, 22.21. Found: C, 66.81; H, 4.85; N, 22.43.

4.1.1.5. 6-(Pyrrolidin-1-yl)phenylpyridazine **7a**

Yield 65 % (0.39 g), mp 135-137˚C. IR: ν_{max}/ cm^{-1} 3044, 2924, 2851, 1605, 1543, 1462. ^{1}H NMR (C*D*Cl$_3$, 400 MHz): δ 2.07-2.11 (m, 4H, pyrrolidine protons), 3.65 (br s, 4H, pyrrolidine protons), 6.80 (d, 1H, *J*= 9.44 Hz, pyridazine proton), 7.38-7.42 (m, 1H, arom. proton), 7.45-7.49 (m, 2H, arom. protons), 7.69 (d, 1H, *J*= 9.48 Hz, pyridazine proton), 8.00-8.06 (m, 2H, arom. protons). ^{13}C NMR (C*D*Cl$_3$, 100 MHz): δ 25.4, 46.9 (pyrrolidine carbons), 119.7, 125.7, 126.3, 127.4, 128.3, 128.7, 129.1, 131.6, 141.8, 149.5 (arom. carbons). MS: m/z (%) 259 (M^+, 69), 261 (M^++2, 23), 70 (100). Anal.Calcd. for $C_{14}H_{15}N_3$ (225.30): C, 74.64; H, 6.71; N, 18.65. Found: C, 74.81; H, 6.79; N, 18.84.

4.1.1.6. 3-(4-Chlorophenyl)-6-(pyrrolidin-1-yl)pyridazine **7b**

Yield 66% (0.39 g), mp 213-215˚C. IR: ν_{max}/ cm^{-1} 3042, 2957, 2855, 1605, 1549, 1487, 1458. ^{1}H NMR (C*D*Cl$_3$, 400 MHz): δ 2.06-2.12 (m, 4H, pyrrolidine protons), 3.63 (br s, 4H, pyrrolidine protons), 6.70 (d, 1H, *J*= 9.48 Hz, pyridazine proton), 7.43 (d, 2H, *J*= 8.52 Hz, arom. protons), 7.58 (d, 1H, *J*= 9.44 Hz, pyridazine proton), 7.94 (d, 2H, *J*= 8.56 Hz, arom. protons). MS: m/z (%) 259 (M^+, 69), 261 (M^++2, 23), 70 (100).

Anal.Calcd. for $C_{14}H_{14}ClN_3$ (259.73): C, 64.74; H, 5.43; N, 16.18. Found: C, 64.85; H, 5.52; N, 16.26.

4.1.1.7. 3-(2-Methoxyphenyl)-6-(pyrrolidin-1-yl)pyridazine **7c**

Yield 57% (0.33 g), mp 130-132˚C. IR: ν_{max}/ cm^{-1} 3055, 2972, 2849, 1603, 1541, 1493, 1470, 1456. ^{1}H NMR (C*D*Cl_3, 400 MHz): δ 1.98-2.01 (m, 4H, pyrrolidine protons), 3.56 (t, 4H, *J*= 6.70 Hz, pyrrolidine protons), 3.77 (s, 3H, OCH_3), 6.64 (d, 1H, *J*= 9.44 Hz, pyridazine proton), 6.91 (d, 1H, *J*= 8.08 Hz, arom. proton), 6.97-7.02 (m, 1H, arom.proton), 7.29 (t, 1H, *J*= 7.20 Hz, arom. proton), 7.73 (d, 1H, *J*= 9.44 Hz, pyridazine proton), 7.85 (dd, 1H, *J*= 1.24, 7.60 Hz, arom. proton). Anal.Calcd. for $C_{15}H_{17}N_3O$ (255.31): C, 70.56; H, 6.71; N, 16.46. Found: C, 70.81; H, 6.78; N, 16.63.

4.1.2. General procedure for the preparation of **8a**–**d**

A solution of the hydrazide derivative **5a**–**d** (2.15 mmol) and acetylacetone (2.30 mmol) in absolute ethanol (5 ml) was heated under reflux for 2 h. The crystals separated on cooling were filtered off, washed and recrystallized from ethanol.

4.1.2.1. 3-(3,5-Dimethyl-1*H*-pyrazol-1-yl)-6-phenylpyridazine **8a**

Yield 41% (0.22 g), mp 109-111˚C (reported 106-107˚C) [54].

4.1.2.2. 3-(4-Chlorophenyl)6-(3,5-dimethyl-1*H*-pyrazol-1-yl)pyridazine **8b**

Yield 60% (0.36 g), mp 177-179˚C (reported 174-175˚C) [55].

4.1.2.3. 3-(3,5-Dimethyl-1*H*-pyrazol-1-yl)-6-(2-methoxyphenyl)pyridazine **8c**

Yield 64% (0.39 g), mp 114-116˚C. IR: ν_{max}/ cm^{-1} 3005, 2978, 2924, 2839, 1605, 1575, 1543, 1435. ^{1}H NMR (C*D*Cl_3, 400 MHz): *δ* 2.34 (s, 3H, CH_3), 2.81 (s, 3H, CH_3), 3.89 (s, 3H, OCH_3), 6.08 (s, 1H, pyrazole proton), 7.05 (d, 1H, *J*= 8.28 Hz, arom. proton), 7.15 (t, 1H, *J*= 7.20 Hz, arom. proton), 7.45-7.49 (m, 1H, arom. proton), 8.01 (dd, 1H, *J*= 1.68, 7.64 Hz, arom. proton), 8.13-8.18 (m, 2H, pyridazine protons. Anal.Calcd. for $C_{16}H_{16}N_4O$ (280.33): C, 68.55; H, 5.75; N, 19.99. Found: C, 68.78; H, 5.83; N, 20.17.

4.1.2.4. 3-(3,5-Dimethyl-1*H*-pyrazol-1-yl)-6-(4-methoxyphenyl)pyridazine **8d**

Yield 65% (0.39 g), mp 148-150˚C. IR: ν_{max}/ cm^{-1} 3003, 2986, 2970, 2924, 2837, 1609, 1571, 1543, 1516, 1468. ^{1}H NMR (C*D*Cl_3, 400 MHz): δ 2.34 (s, 3H, CH_3), 2.82 (s, 3H, CH_3), 3.90 (s, 3H, OCH_3), 6.09 (s, 1H, pyrazole proton), 7.06 (d, 2H, *J*= 8.84 Hz, arom. proton), 7.92 (d, 1H, *J*= 9.28 Hz, pyridazine proton), 8.08 (d, 2H, *J*= 8.84 Hz, arom. protons), 8.18 (d, 1H, *J*= 9.28 Hz, pyridazine proton). ^{13}C NMR ($CDCl_3$, 100 MHz): δ 13.7 (CH_3), 15.0 (CH_3), 55.4 (OCH_3), 110.0, 114.4, 120.5, 125.5, 128.2, 128.3, 142.4, 151.2, 155.4, 156.6, 161.3 (arom. carbons). Anal.Calcd. for $C_{16}H_{16}N_4O$ (280.33): C, 68.55; H, 5.75; N, 19.99. Found: C, 68.82; H, 5.81; N, 20.23.

4.1.3. General procedure for the preparation of **9a**–**d** and **10a**–**d**

An equimolar mixture of the hydrazine derivative **5a-d** and ethoxymethylene malononitrile or ethyl ethoxymethylene cyanoacetate (2.30 mmol) in absolute ethanol (5ml) was refluxed for 2 h. The formed precipitate was filtered off on hot and washed with ethanol to give **9a-d** or **10a-d**, respectively in pure form.

4.1.3.1. 5-Amino-1-(6-phenylpyridazin-3-yl)-1*H*-pyrazole-4-carbonitrile **9a**

Yield 84% (0.51 g), mp 254-255˚C (reported 251-252˚C) [56].

4.1.3.2. 5-Amino-1-[6-(4-chlorophenyl)pyridazin-3-yl]-1*H*-pyrazole-4-carbonitrile **9b**

Yield 75% (0.51 g), mp 294-296˚C. IR: ν_{max}/ cm^{-1} 3397, 3294, 3078, 3063, 2230, 1622, 1595, 1560, 1551, 1524, 1493. ^{1}H NMR (DMSO-d_6, 400 MHz): δ 7.65 (d, 2H, *J*= 8.60 Hz, arom. protons), 8.04 (s, 1H, pyrazole proton), 8.19-8.23 (m, 3H, 2 arom. protons + pyridazine proton), 8.26 (s, 2H, NH_2 exchanged with D_2O), 8.49 (d, 1H, *J*= 9.40 Hz, pyridazine proton). ^{13}C NMR (DMSO-d_6, 100 MHz): δ 74.1 (*C*-CN), 114.6 (CN), 120.0, 128.4, 129.0, 130.0, 134.4, 135.7, 144.4, 153.6, 156.1, 156.8 (arom. carbons). Anal.Calcd. for $C_{14}H_9ClN_6$ (296.72): C, 56.67; H, 3.06; N, 28.32. Found: C, 56.84; H, 3.04; N, 28.49.

4.1.3.3. 5-Amino-1-[6-(2-methoxyphenyl)pyridazin-3-yl]-1*H*-pyrazole-4-carbonitrile **9c**
Yield 69% (0.47 g), mp 266-268˚C. IR: ν_{max}/ cm^{-1} 3387, 3285, 3096, 3082, 3069, 3007, 2980, 2947, 2918, 2839, 2218, 1636, 1603, 1584, 1549, 1524, 1495. ^{1}H NMR (DMSO-d_6, 400 MHz): δ 3.86 (s, 3H, OCH_3), 7.14 (t, 1H, *J*= 7.46 Hz, arom. proton), 7.23 (d, 1H, *J*= 8.32 Hz, arom. proton), 7.53 (t, 1H, *J*= 7.44 Hz, arom. proton), 7.79 (d, 1H, *J*= 7.24 Hz, arom. proton), 8.02 (s, 1H, pyrazole proton), 8.16 (d, 1H, *J*= 9.32 Hz, pyridazine proton), 8.25 (s, 2H, NH_2 exchanged with D_2O), 8.28 (d, 1H, *J*= 9.40 Hz, pyridazine proton). Anal.Calcd. for $C_{15}H_{12}N_6O$ (292.30): C, 61.64; H, 4.14; N, 28.75. Found: C, 61.87; H, 4.19; N, 28.93.

4.1.3.4. 5-Amino-1-[6-(4-methoxyphenyl)pyridazin-3-yl]-1*H*-pyrazole-4-carbonitrile **9d**
Yield 97% (0.65 g), mp 294-295˚C. IR: ν_{max}/ cm^{-1} 3397, 3296, 3078, 3038, 3005, 2970, 2918, 2843, 2210, 1622, 1605, 1580, 1551, 1512, 1449. ^{1}H NMR (DMSO-d_6, 400 MHz): δ 3.85 (s, 3H, OCH_3), 7.13 (d, 2H, *J*= 8.80 Hz, arom. protons), 8.02 (s, 1H, pyrazole proton), 8.13-8.17 (m, 3H, 2 arom. protons + pyridazine proton), 8.23 (s, 2H, NH_2 exchanged with D_2O), 8.42 (d, 1H, *J*= 9.40 Hz, pyridazine proton). Anal.Calcd. for $C_{15}H_{12}N_6O$ (292.30): C, 61.64; H, 4.14; N, 28.75. Found: C, 61.83; H, 4.21; N, 28.97.

4.1.3.5. Ethyl 5-amino-1-(6-phenylpyridazin-3-yl)-1*H*-pyrazole-4-carboxylate **10a**
Yield 79% (0.56 g), mp 188-190˚C (reported 190-191˚C) [57].

4.1.3.6. Ethyl 5-amino-1-[6-(4-chlorophenyl)pyridazin-3-yl]-1*H*-pyrazole-4-carboxylate **10b**
Yield 68% (0.54 g), mp 209-211˚C. IR: ν_{max}/ cm^{-1} 3443, 3333, 3084, 3073, 2986, 2941, 2916, 2903, 1674, 1607, 1593, 1541, 1493. ^{1}H NMR (C*D*Cl_3, 400 MHz): δ 1.39 (t, 3H, *J*= 7.12 Hz, CH_3), 4.34 (q, 2H, *J*= 7.12 Hz, CH_2), 7.53 (d, 2H, *J*= 8.48 Hz, arom. protons), 7.61 (s, 2H, NH_2 exchanged with D_2O), 7.84 (s, 1H, pyrazole proton), 7.98-8.02 (m, 3H, 2 arom. protons + pyridazine proton), 8.26 (d, 1H, *J*= 9.32 Hz, pyridazine proton). ^{13}C NMR (C*D*Cl_3, 75 MHz): δ 14.4 (CH_3), 59.6 (OCH_2), 119.0, 125.8, 126.4, 127.9, 129.3, 133.8, 136.5, 138.4, 142.7, 152.0, 155.8 (arom. carbons), 164.0 (C=O). MS

(m/z, %): 343 (M^+, 100), 344 [M^++ 1], 297 (50). Anal.Calcd. for $C_{16}H_{14}ClN_5O_2$ (343.77): C, 55.90; H, 4.11; N, 20.37. Found: C, 56.07; H, 4.15; N, 20.49.

4.1.3.7. Ethyl 5-amino-1-[6-(2-methoxyphenyl)pyridazin-3-yl]-1*H*-pyrazole-4-carboxylate **10c**

Yield 64% (0.50 g), mp 137-139˚C. IR: ν_{max}/ cm^{-1} 3424, 3312, 3080, 2990, 2959, 2918, 2839, 1688, 1618, 1601, 1545, 1493. ^{1}H NMR (C*D*Cl_3, 400 MHz): δ 1.37 (t, 3H, *J*= 7.12 Hz, CH_3), 3.87 (s, 3H, OCH_3), 4.31 (q, 2H, *J*= 7.10 Hz, CH_2), 7.03 (d, 1H, *J*= 8.32 Hz, arom. proton), 7.12 (t, 1H, *J*= 7.48 Hz, arom. proton), 7.41 (t, 1H, *J*= 8.48 Hz, arom. proton), 7.62 (s, 2H, NH_2 exchanged with D_2O), 7.82 (s, 1H, pyrazole proton), 7.90 (dd, 1H, *J*= 1.24, 7.60 Hz, arom. proton), 8.14 (s, 2H, pyridazine protons). ^{13}C NMR (C*D*Cl_3, 100 MHz): δ 14.6 (CH_3), 55.6 (OCH_3), 59.7 (CH_2), 95.5, 111.4, 117.5, 121.3, 125.0, 130.5, 130.8, 131.3, 142.5, 152.1, 156.2, 156.5, 157.1 (arom. carbons), 164.2 (C=O). Anal.Calcd. for $C_{17}H_{17}N_5O_3$ (339.36): C, 60.17; H, 5.05; N, 20.64. Found: C, 60.34; H, 5.08; N, 20.87.

4.1.3.8. Ethyl 5-amino-1-[6-(4-methoxyphenyl)pyridazin-3-yl]-1*H*-pyrazole-4-carboxylate **10d**

Yield 79% (0.62 g), mp 198-200˚C. IR: ν_{max}/ cm^{-1} 3453, 3331, 3082, 3046, 2988, 2965, 2922, 2901, 2833, 1676, 1612, 1580, 1545, 1516. ^{1}H NMR (C*D*Cl_3, 400 MHz): δ 1.39 (t, 3H, *J*= 7.12 Hz, CH_3), 3.90 (s, 3H, OCH_3), 4.33 (q, 2H, *J*= 7.12 Hz, CH_2), 7.06 (d, 2H, *J*= 8.84 Hz, arom. protons), 7.60 (br s, 2H, NH_2 exchanged with D_2O), 7.84 (s, 1H, pyrazole proton), 7.96 (d, 1H, *J*= 9.36 Hz, pyridazine proton), 8.02 (d, 2H, *J*= 8.84 Hz, arom. protons), 8.20 (d, 1H, *J*= 9.36 Hz, pyridazine proton). ^{13}C NMR (C*D*Cl_3, 75 MHz): δ 14.4 (CH_3), 55.3 (OCH_3), 59.6 (OCH_2), 114.5, 118.9, 126.1, 127.8, 128.1, 142.4, 151.9, 156.2, 156.5, 161.4 (arom. carbons), 164.1 (C=O). Anal.Calcd. for $C_{17}H_{17}N_5O_3$ (339.36): C, 60.17; H, 5.05; N, 20.64. Found: C, 60.31; H, 5.12; N, 20.91.

4.1.4. General procedure for the preparation of **11a–c**

To a mixture of the hydrazine derivative **5b,c** (1.65 mmol) and triethylamine (0.25 ml) in dry methylene chloride (5 ml), the appropriate isocyanate (1.65 mmol) was added

dropwise. The reaction was stirred at room temperature for 6 h, the obtained precipitate was filtered off, washed and crystallized from ethanol.

4.1.4.1. 2-[6-(4-Chlorophenyl)pyridazin-3-yl]-*N*-cyclohexylhydrazine-1-carboxamide **11a**

Yield 43% (0.24 g), mp 211-213˚C. IR: ν_{max}/ cm^{-1} 3300, 3242, 3134, 3051, 3034, 3015, 2930, 2853, 1645, 1614, 1601, 1558, 1464. ^{1}H NMR (C*D*Cl$_3$, 400 MHz): δ 1.01-1.09 (m, 2H, cyclohexyl protons), 1.23-1.33 (m, 2H, cyclohexyl protons), 1.51-1.64 (m, 4H, cyclohexyl protons), 1.85 (br d, 2H, *J*= 9.4 Hz, cyclohexyl protons), 3.56-3.66 (m, 1H, cyclohexyl proton), 5.59 (s, 1H, NH exchanged with D_2O), 5.61 (s, 1H, NH exchanged with D_2O), 6.77 (s, 1H, NH exchanged with D_2O), 7.13 (d, 1H, *J*= 9.24 Hz, pyridazine proton), 7.42 (d, 2H, *J*= 8.68 Hz, arom. protons), 7.66 (d, 1H, *J*= 9.24 Hz, pyridazine proton), 7.81 (d, 2H, *J*= 8.28 Hz, arom. protons). Anal.Calcd. for $C_{17}H_{20}ClN_5O$ (345.83): C, 59.04; H, 5.83; N, 20.25. Found: C, 59.25; H, 5.91; N, 20.41.

4.1.4.2. *N*-Cyclohexyl-2-[6-(2-methoxyphenyl)pyridazin-3-yl]hydrazine-1-carboxamide **11b**

Yield 74% (0.42 g), mp 197-198˚C. IR: ν_{max}/ cm^{-1} 3306, 3223, 3073, 2999, 2928, 2853, 1659, 1599, 1580, 1541, 1493, 1460. ^{1}H NMR (C*D*Cl$_3$, 400 MHz): δ 1.08 (td, 2H, *J*= 2.87, 11.89, 14.80 Hz, cyclohexyl protons), 1.21-1.31 (m, 2H, cyclohexyl protons), 1.50-1.56 (m, 2H, cyclohexyl protons), 1.61-1.65 (m, 2H, cyclohexyl protons), 1.85 (dd, 2H, *J*= 2.92, 12.16 Hz, cyclohexyl protons), 3.53-3.61 (m, 1H, cyclohexyl proton), 3.78 (s, 3H, OCH_3), 3.81 (s, 1H, NH exchanged with D_2O), 3.82 (s, 1H, NH exchanged with D_2O), 5.95 (s, 1H, NH exchanged with D_2O), 6.94 (d, 1H, *J*= 8.32 Hz, arom. proton), 7.02 (td, 1H, *J*= 0.83, 7.53, 8.33 Hz), 7.20 (d, 1H, *J*= 9.24 Hz, pyridazine proton), 7.36 (td, 1H, *J*= 1.74, 7.86, 9.12), 7.70 (dd, 1H, *J*= 1.64, 7.60 Hz, arom.proton), 7.88 (d, 1H, *J*= 9.32 Hz, pyridazine proton. ^{13}C NMR (C*D*Cl$_3$, 75 MHz): δ 24.8, 25.4, 33.5, 48.7 (cyclohexyl carbons), 55.4 (OCH_3), 111.2, 112.0, 121.1, 125.7, 130.5, 130.7, 138.5, 156.8, 160.0 (arom. carbons), 158.1 (C=O). Anal.Calcd. for $C_{18}H_{23}N_5O_2$ (341.42): C, 63.32; H, 6.79; N, 20.51. Found: C, 63.48; H, 6.85; N, 20.67.

4.1.4.3. 2-[6-(4-Chlorophenyl)pyridazin-3-yl]-*N*-phenylhydrazine-1-carboxamide **11c**

Yield 64% (0.35 g), mp 237-239˚C. IR: ν_{max}/ cm^{-1} 3329, 3250, 3138, 3061, 3007, 2984, 1659, 1601, 1597, 1557, 1448. ^{1}H NMR (DMSO-d_6, 400 MHz): δ 6.95 (t, 1H, *J*=7.34Hz, arom. proton), 7.08 (d, 1H, *J*= 9.36 Hz, pyridazine proton), 7.25 (t, 2H, *J*= 7.94 Hz, arom. protons), 7.51 (d, 2H, *J*= 7.92 Hz, arom. protons), 7.56 (d, 2H, *J*= 8.64 Hz, arom. protons), 8.02 (d, 1H, *J*= 9.36 Hz, pyridazine proton), 8.05 (d, 2H, *J*= 8.68 Hz, arom. protons), 8.34 (s, 1H, NH exchanged with D_2O), 8.91 (s, 1H, NH exchanged with D_2O), 8.96 (s, 1H, NH exchanged with D_2O). ^{13}C NMR (DMSO-d_6, 75 MHz): δ 113.2, 118.6, 121.8, 125.6, 127.4, 128.5, 128.8, 135.5, 139.6, 151.1, 160.5 (arom. carbons), 156.1 (C=O). Anal.Calcd. for $C_{17}H_{14}ClN_5O$ (339.78): C, 60.09; H, 4.15; N, 20.61. Found: C, 60.18; H, 4.19; N, 20.89.

4.1.5. General procedure for the preparation of **12a**–**h**

To an equimolar mixture of the hydrazine derivative **5b,c** and the appropriate aldehyde in absolute ethanol (25ml) was added glacial acetic acid (0.50 ml). The reaction was heated under reflux for 3 h. The obtained precipitate was filtered off and washed with ethanol to give **12a**–**h** in a pure form.

4.1.5.1. 3-(4-Chlorophenyl)-6-{2-[4-(trifluoromethyl)benzylidene]hydrazinyl}pyridazine **12a**

Yield 87% (0.59 g), mp > 300˚C. IR: ν_{max}/ cm^{-1} 3120, 3050, 1611, 1593, 1549, 1489. ^{1}H NMR (DMSO-d_6, 400 MHz): δ 7.59 (d, 2H, *J*= 7.04 Hz, arom. protons), 7.72-7.79 (m, 3H, 2 arom. protons + pyridazine proton), 7.95 (d, 2H, *J*= 7.24 Hz, arom. protons), 8.11-8.16 (m, 3H, 2 arom. protons + pyridazine proton), 8.23 (s, 1H, N=CH), 11.93 (s, 1H, NH exchanged with D_2O). Anal.Calcd. for $C_{18}H_{12}ClF_3N_4O$ (376.76): C, 57.38; H, 3.21; N, 14.87. Found: C, 57.49; H, 3.23; N, 15.01.

4.1.5.2. 3-(4-Methoxyphenyl)-6-{2-[4-(trifluoromethyl)benzylidene]hydrazinyl} pyridazine **12b**

Yield 77% (0.53 g), mp 262-264˚C. IR: ν_{max}/ cm^{-1} 3125, 3060, 2940, 2839, 1611, 1589, 1545, 1493. ^{1}H NMR (C*D*Cl$_3$, 400 MHz): δ 3.83 (s, 3H, OCH_3), 6.98 (d, 1H, arom.

proton), 7.05 (t, 1H, *J*= 7.50 Hz, arom. protons), 7.42 (t, 1H, *J*= 7.74 Hz, arom. protons), 7.60 (d, 3H, *J*= 7.84 Hz, arom. protons+ pyridazine proton), 7.70 (d, 1H, *J*= 6.64 Hz, arom. proton), 7.77 (d, 2H, *J*= 7.92 Hz, arom. protons), 7.95 (s, 1H, NH, exchanged with D_2O), 8.09 (d, 1H, *J*= 9.12 Hz, pyridazine proton), 8.39 (s, 1H, N=CH). Anal.Calcd. for $C_{19}H_{15}F_3N_4O$ (372.34): C, 61.29; H, 4.06; N, 15.05. Found: C, 61.43; H, 4.12; N, 15.23.

4.1.5.3. 3-(4-Chlorophenyl)-6-[2-(4-methoxybenzylidene)hydrazinyl]pyridazine **12c**
Yield 82% (0.63 g), mp 272-273˚C. IR: ν_{max}/ cm^{-1} 3125, 3060, 2951, 2916, 2835, 1618, 1603, 1551, 1508, 1489. ^{1}H NMR (DMSO-d_6, 400 MHz): δ 3.81 (s, 3H, OCH_3), 7.00 (d, 2H, *J*= 7.36 Hz, arom. proton), 7.56-7.68 (m, 5H, arom. protons), 8.09 (d, 4H, *J*= 8.28 Hz, arom. protons + N=CH), 11.53 (s, 1H, NH, exchanged with D_2O). Anal.Calcd. for $C_{18}H_{15}ClN_4O$ (338.79): C, 63.81; H, 4.46; N, 16.54. Found: C, 63.96; H, 4.53; N, 16.80.

4.1.5.4. 3-[2-(4-Methoxybenzylidene)hydrazinyl] 6-(4-methoxyphenyl)pyridazine **12d**
Yield 80% (0.62 g), mp 239-241˚C. IR: ν_{max}/ cm^{-1} 3120, 3005, 2930, 2906, 2831, 1611, 1593, 1541, 1508, 1493. ^{1}H NMR (DMSO-d_6, 400 MHz): δ 3.81 (s, 3H, OCH_3), 3.84 (s, 3H, OCH_3), 7.00 (d, 2H, *J*= 8.64 Hz, arom. protons), 7.09 (t, 1H, *J*= 7.38 Hz, arom. proton), 7.17 (d, 1H, *J*= 8.24 Hz, arom. proton), 7.43 (t, 1H, *J*= 7.16 Hz, arom. proton), 7.57 (d, 1H, *J*= 9.32 Hz, pyridazine proton), 7.65 (d, 2H, *J*= 8.64 Hz, arom. protons), 7.71 (d, 1H, *J*= 6.44 Hz, arom. proton), 7.86 (d, 1H, *J*= 9.36 Hz, pyridazine proton), 8.11 (s, 1H, N=CH), 11.40 (s, 1H, NH, exchanged with D_2O). ^{13}C NMR (DMSO-d_6, 75 MHz): δ 55.2 (OCH_3), 55.6 (OCH_3), 111.0, 111.8, 114.2, 120.5, 126.2, 128.2, 129.7, 141.0, 151.5, 156.5, 158.0, 160.0 (arom. carbons). Anal.Calcd. for $C_{19}H_{18}N_4O_2$ (334.38): C, 68.25; H, 5.43; N, 16.76. Found: C, 68.47; H, 5.49; N, 16.94.

4.1.5.5. 3-(4-Chlorophenyl)-6-[2-(2,4-dimethoxybenzylidene)hydrazinyl]pyridazine **12e**
Yield 79% (0.53 g), mp 225-226˚C. IR: ν_{max}/ cm^{-1} 3150, 3003, 2968, 2940, 2928, 2835, 1609, 1568, 1539, 1504, 1489. ^{1}H NMR (C*D*Cl_3, 400 MHz): δ 3.77 (s, 3H, OCH_3), 3.79 (s, 3H, OCH_3), 6.39 (d, 1H, *J*= 1.96 Hz, arom. proton), 6.48 (dd, 1H, *J*= 1.86, 8.66 Hz, arom. proton), 7.39 (d, 2H, *J*= 8.48 Hz, arom. protons), 7.70-7.87 (m, 6H, 2 pyridazine

protons + 3 arom. protons + NH exchanged with D_2O), 8.43 (s, 1H, N=CH). ^{13}C NMR ($CDCl_3$, 100 MHz): δ 55.5 (OCH_3), 55.6 (OCH_3), 98.1, 105.8, 116.1, 126.5, 127.1, 127.4, 129.1, 135.2, 140.3, 145.0, 153.5, 156.5, 157.0 (arom. carbons). Anal.Calcd. for $C_{19}H_{17}ClN_4O_2$ (368.82): C, 61.87; H, 4.65; N, 15.19. Found: C, 62.13; H, 4.69; N, 15.35.

4.1.5.6. 3-[2-(2,4-Dimethoxybenzylidene)hydrazinyl]-6-(2-methoxyphenyl)pyridazine **12f**

Yield 72% (0.48 g), mp 214-216˚C. IR: ν_{max}/ cm^{-1} 3200, 3013, 3003, 2955, 2918, 2897, 2833, 1607, 1566, 1539, 1503, 1491. ^1H NMR ($CDCl_3$, 400 MHz): δ 3.73 (s, 3H, OCH_3), 3.78 (s, 3H, OCH_3), 3.80 (s, 3H, OCH_3), 6.38 (d, 1H, *J*= 2.20 Hz, arom. proton), 6.47 (dd, 1H, *J*= 2.16, 8.64 Hz, arom. proton), 6.94 (d, 1H, *J*= 8.28 Hz, arom. proton), 7.02 (t, 1H, *J*= 7.46 Hz, arom. proton), 7.31-7.35 (m, 1H, arom. proton), 7.59 (d, 1H, *J*= 9.40 Hz, pyridazine proton), 7.81-7.84 (m, 4H, pyridazine proton + 2 arom. protons + NH exchanged with D_2O), 8.36 (s, 1H, N=CH). ^{13}C NMR ($CDCl_3$, 75 MHz): δ 55.3 (OCH_3), 55.4 (OCH_3), 55.5 (OCH_3), 98.1, 105.4, 111.2, 112.1, 117.0, 121.0, 125.8, 126.8, 129.7, 130.5, 130.6, 138.2, 151.8, 156.9, 158.4, 158.7, 161.6 (arom. carbons). Anal.Calcd. for $C_{20}H_{20}N_4O_3$ (364.41): C, 65.92; H, 5.53; N, 15.38. Found: C, 66.11; H, 5.64; N, 15.52.

4.1.5.7. 3-(4-Chlorophenyl)-6-[2-(3,4,5-trimethoxybenzylidene)hydrazinyl]pyridazine **12g**

Yield 83% (0.60 g), mp 294-296˚C. IR: ν_{max}/ cm^{-1} 3219, 3086, 2997, 2924, 2851, 2833, 1614, 1599, 1539, 1506, 1491. ^1H NMR (DMSO-d_6, 400 MHz): δ 3.70 (s, 3H, OCH_3), 3.86 (s, 6H, $2OCH_3$), 7.03 (s, 2H, arom. protons), 7.57 (d, 2H, *J*=8.16 Hz, arom. protons), 7.70 (d, 1H, *J*= 9.36 Hz, pyridazine proton), 8.08-8.10 (m, 4H, pyridazine proton + 2 arom. protons + N=CH), 11.70 (s, 1H, NH exchanged with D_2O). Anal.Calcd. for $C_{20}H_{19}ClN_4O_3$ (398.85): C, 60.23; H, 4.80; N, 14.05. Found: C, 60.47; H, 4.87; N, 14.13.

4.1.5.8. 3-(2-Methoxyphenyl)-6-[2-(3,4,5-trimethoxybenzylidene)hydrazinyl]pyridazine **12h**

Yield 75% (0.55 g), mp 252-254˚C. IR: ν_{max}/ cm^{-1} 3200, 3086, 2997, 2955, 2926, 2837, 1601, 1589, 1576, 1506, 1491. ^1H NMR ($CDCl_3$, 400 MHz): δ 3.81 (s, 6H, $2OCH_3$), 3.82

(s, 6H, 2OCH_3), 6.88 (s, 2H, arom. protons), 6.97 (d, 1H, *J*= 8.32 Hz, arom. proton), 7.02 (t, 1H, *J*= 7.48 Hz, arom. proton), 7.36 (t, 1H, *J*= 7.14 Hz, arom. proton), 7.68 (d, 1H, *J*= 9.40 Hz, pyridazine proton), 7.84 (d, 2H, arom. proton + NH exchanged with D_2O), 7.91 (d, 1H, J= 9.40 Hz, pyridazine proton), 8.38 (s, 1H, N=CH). ^{13}C NMR ($CDCl_3$, 75 MHz): δ 55.5 (OCH_3), 56.0 (OCH_3), 60.8(OCH_3), 94.6, 103.5, 111.4, 112.2, 120.8, 130.0, 130.3, 130.8, 130.9, 143.2, 144.2, 153.4, 157.5 (arom. carbons). Anal.Calcd. for $C_{21}H_{22}N_4O_4$ (394.42): C, 63.95; H, 5.62; N, 14.20. Found: C, 64.12; H, 5.69; N, 14.37.

4.2. Vasorelaxant activity

The vasorelaxant activity screening procedure was carried out according to the standard reported techniques [34–40] by testing the effects of the synthesized compounds **5a–d, 6a–d**, **7a–c**, **8a–d, 9a–d, 10a–d**, **11a–c**, **12a–h** and the reference standard, doxazosin mesylate, on isolated thoracic aortic rings of male Wister rats (250-350 g). After light ether anesthesia, the rats were sacrificed by cervical dislocation.

The aorta was immediately excised, freed of extraneous tissues and prepared for isometric tension recording. Aorta was cut into (3-5 mm width) rings and each ring was placed in a vertical chamber "10 ml jacketed automatic multi-chamber organ bath system (Model no. ML870B6/C, Panlab, Spain)" filled with Krebs solution composed of (in mM): NaCl, 118.0; KCl, 4.7; $NaHCO_3$, 25.0; $CaCl_2$, 1.8; NaH_2PO_4, 1.2; $MgSO_4$, 1.2; glucose, 11.0 and oxygenated with carbogen gas (95% O_2/5% CO_2) at 37+0.5˚C. Each aortic ring was mounted between two stainless steel hooks passed through its lumen. The lower hook was fixed between two plates, while the upper one was attached to a force displacement transducer (Model no. MLT0201, Panlab, Spain) connected to an amplifier (PowerLab, AD Instruments Pty. Ltd.) which is connected to a computer. The Chart for windows (v 3.4) software was used to record and elaborate data.

Preparations were stabilized under 2 g resting tension during 2 h and then the contracture response to norepinephrine hydrochloride (10^{-6} M) was measured before and after exposure to increasing concentrations of the tested synthesized compounds.

The tested compounds were dissolved in dimethylsulfoxide (DMSO) as stock solution (10 ml of 0.01 M). Control experiments were performed in the presence of DMSO alone, at the same concentrations as those used with the derivatives tested, which demonstrated

that the solvent did not affect the contractile response of isolated aorta. The observed vasodilatation activity screening data were reported (Table 1) and the potency (IC_{50}, concentration necessary for 50% reduction of maximal norepinephrine hydrochloride induced contracture) was determined by the best-fit line technique.

Acknowledgment

The author is thankful to Prof. Adel S. Girgis, Pesticide Chemistry Department, National Research Centre, Dokki, Cairo 12622, Egypt, for his assistance in performing the QSAR study.

References

[1] C. Kennedy, The importance of drug discovery for treatment of cardiovascular diseases, Future Med. Chem. 5 (2013) 355–357.

[2] A.E. Kümmerle, J.M. Raimundo, C.M. Leal, G.S. daSilva, T.L. Balliano, M.A. Pereira, C.A. de Simone, R.T. Sudo, G. Zapata-Sudo, C.A.M. Fraga, E.J. Barreiro, Studies towards the identification of putative bioactive conformation of potent vasodilator arylidene *N*-acylhydrazone derivatives, Eur. J. Med. Chem. 44 (2009) 4004–4009.

[3] A.S. Go, D. Mozaffarian, V.L. Roger, E.J. Benjamín, J.D. Berry, W.B. Borden, Heart disease and stroke statistics—2013 update a report from the American Heart Association, Circulation 127 (2013) e6–e245.

[4] M.E. Ernst, M. Moser, Use of diuretics in patients with hypertension, N. Engl. J. Med. 361 (2009) 2153–2164.

[5] R. Donnelly, Angiotensin-converting enzyme inhibitors and coronary heart disease prevention, J. Renin Angiotensin Aldosterone Syst. 8 (2007) 13–22.

[6] H.T. Ong, Are Angiotensin-converting enzyme inhibitors and angiotensin receptor blockers especially useful for cardiovascular protection?, J. Am. Board Fam. Med. 22 (2009) 686–697.

[7] F.H. Messerli, S. Bangalore, F. Ruschitzka, Angiotensin receptor blockers: baseline therapy in hypertension, Eur. Heart J. 30 (2009) 2427–2430.

[8] M. Pahor, B.M. Psaty, W.B. Alderman, W.B. Applegate, J.D. Williamson, C. Cavazzini, C.D. Furberg, Health outcomes associated with calcium antagonists

compared with other first-line antihypertensive therapies: a meta-analysis of randomised controlled trials, Lancet 356 (2000) 1949–1954.

[9] B. Szabo, Imidazoline antihypertensive drugs: a critical review on their mechanism of action, Pharmacol. Ther. 93 (2002) 1–35.

[10] L.H. Lindholm, B. Carlberg, O. Samuelsson, Should β blockers remain first choice in the treatment of primary hypertension? A meta-analysis, Lancet 366 (2005) 1545–1553.

[11] L. Kalinowski, L.W. Dobrucki, M. Szczepanska-Konkel, M. Jankowski, L. Martyniec, S. Angielski, T. Malinski, Third-generation β-blockers stimulate nitric oxide release from endothelial cells through ATP efflux: A novel mechanism for antihypertensive action, Circulation 107 (2003) 2747–2752.

[12] A.T. Remaley, Old drug, new tricks: The unexpected effect of doxazosin on high-density lipoprotein, Circulation Res. 101 (2007) 116–118.

[13] G.S. Stokes, Systolic hypertension in the elderly: Pushing the frontiers of therapy—A suggested new approach, J. Clin. Hypertens. 6 (2004) 192–197.

[14] H. Marona, N. Szkaradek, A. Rapacz, B. Filipek, M. Dybata, A. Siwek, M. Cegta, E. Szneler, Preliminary evaluation of pharmacological properties of some xanthone derivatives, Bioorg. Med. Chem. 17 (2009) 1345–1352.

[15] J.-M. Contreras, I. Parrot, W. Sippl, Y.M. Rival, C.G. Wermuth, Design, synthesis, and structure−activity relationships of a series of 3-[2-(1-benzylpiperidin-4-yl)ethylamino]pyridazine derivatives as acetylcholinesterase inhibitors, J. Med. Chem. 44 (2001) 2707–2718.

[16] T.C. Ramalho, M. Rocha, E. da Cunha, M.P. Freitas, The search for new COX-2 inhibitors: a review of 2002 – 2008 patents, Expert Opin. Ther. Patents 19 (2009) 1–36.

[17] A. Coelho, E. Raviña, N. Fraiz, M. Yáñez, R. Laguna, E. Cano, E. Sotelo, Design, synthesis, and structure–activity relationships of a novel series of 5-alkylidenepyridazin-3(2*H*)-ones with a non-cAMP-based antiplatelet activity, J. Med. Chem. 50 (2007) 6476–6484.

[18] C. Biancanali, M.P. Giovannoni, S. Pieretti, N. Cesari, A. Graciano, C. Vergelli, A. Cilibrizzi, A. di Gianuario, M. Colucci, G. Mangano, B. Garrone, L. Polenzani, V. dal Piaz, Further studies on arylpiperazinyl alkyl pyridazinones: Discovery of an exceptionally potent, orally active, antinociceptive agent in thermally induced pain, J.

Med. Chem. 52 (2009) 7397–7409.

[19] J.A. Bristol, I. Sircar, W.H. Moos, D.B. Evans, R.E. Weishaar, Cardiotonic agents. 1. 4,5-Dihydro-6-[4-(1*H*-imidazol-1-yl)phenyl]-3(2*H*)-pyridazinones: novel positive inotropic agents for the treatment of congestive heart failure, J. Med. Chem. 27 (1984) 1099–1101.

[20] W.H. Moos, C.C. Humblet, I. Sircar, C. Rithner, R.E. Weishaar, J.A. Bristol, A.T. McPhail, Cardiotonic agents. 8. Selective inhibitors of adenosine 3',5'-cyclic phosphate phosphodiesterase III. Elaboration of a five-point model for positive inotropic activity, J. Med. Chem. 30 (1987) 1963–1972.

[21] S. Demirayak, A.C. Karaburun, R. Beis, Some pyrrole substituted aryl pyridazinone and phthalazinone derivatives and their antihypertensive activities**,** Eur. J. Med. Chem. 39 (2004)1089–1095.

[22] K. Abouzid, M.A. Hakeem, O. Khalil, Y. Maklad, Pyridazinone derivatives: Design, synthesis, and in vitro vasorelaxant activity, Bioorg. Med. Chem. 16 (2008) 382–389.

[23] C. Schudt, S. Winder, B. Müller, D. Ukena, Zardaverine as a selective inhibitor of phosphodiesterase isozymes, Biochem. Pharmacol. 42 (1991) 153–162.

[24] S. Corsano, R. Vezza, R. Scapicchi, S. Foresi, G. Strappaghetti, G.G. Nenci, P. Gresele, New pyridazinone derivatives as inhibitors of platelet aggregation, Eur. J. Med. Chem. 30 (1995) 627–631.

[25] M. Asif, Some recent approaches of biologically active substituted pyridazine and phthalazine drugs, Curr. Med. Chem. 19 (2012) 2984–2991.

[26] R.E. Weishaar, M.H. Cain, J.A. Bristol, A new generation of phosphodiesterase inhibitors: Multiple molecular forms of phosphodiesterase and the potential for drug selectivity, J. Med. Chem. 28 (1985) 537–545.

[27] W.J. Coates, H.D. Prain, M.L. Reeves, B.H. Warrington, 1,4-Bis(3-oxo-2,3-dihydropyridazin-6-yl)benzene analogs: potent phosphodiesterase inhibitors and inodilators, J. Med. Chem. 33 (1990) 1735–1741.

[28] J. Druey, A. Marxer, Hypotensive hydrazinophthalazines and related compounds, J. Med. Pharm. Chem. 1 (1) (1959) 1–21.

[29] A.A. Siddiqui, R. Mishra, M. Shaharyar, Synthesis, characterization and antihypertensive activity of pyridazinone derivatives, Eur. J. Med. Chem. 45 (2010)

2283–2290.

[30] R. Bansal, D. Kumar, R. Carron, C. de la Calle, Synthesis and vasodilatory activity of some amide derivatives of 6-(4-carboxymethyloxyphenyl)-4,5-dihydro-3(2*H*)-pyridazinone, Eur. J. Med. Chem. 44 (2009) 4441–4447.

[31] J.O. Aldaa , M.S. Valeroa , D. Perebooma , P. Grosa, R.P. Garay, Endothelium-independent vasorelaxation by the selective alpha estrogen receptor agonist propyl pyrazole triol in rat aortic smooth muscle, J. Pharm. Pharmacol. 61 (2009) 641–646.

[32] W.J. Coates, A. McKillop, One-pot preparation of 6-substituted 3 (2*H*)-pyridazinones from ketones, Synthesis (1993)334–342.

[33] A.E. Kümmerle, M.M. Vieira, M. Schmit, A.L.P. Miranda, C.A.M. Fraga, J.-J. Bourguignon, E.J. Barreiro, Design, synthesis and analgesic properties of novel conformationally-restricted *N*-acylhydrazones (NAH), Bioorg. Med. Chem. Lett. 19 (2009) 4963–4966**.**

[34] A.S. Girgis, A. Kalmouch, M. Ellithey, Synthesis of novel vasodilatory active nicotinate esters with amino acid function, Bioorg. Med. Chem. 14 (2006) 8488−8494.

[35] A.S. Girgis, N. Mishriky, A.M. Farag, W.I. El-Eraky, H. Farag**,** Synthesis of new 3-pyridinecarboxylates of potential vasodilation properties, Eur. J. Med. Chem. 43 (2008) 1818−1827.

[36] A.S. Girgis, N.S.M. Ismail, H. Farag, W.I. El-Eraky, D.O. Saleh, S.R. Tala, A.R. Katritzky, Regioselective synthesis and molecular modeling study of vasorelaxant active 7,9-dioxa-1,2-diaza-spiro[4.5]dec-2-ene-6,10-diones, Eur. J. Med. Chem. 45 (2010) 4229−4238.

[37] A.S. Girgis, N.S.M. Ismail, H. Farag, Facile synthesis, vasorelaxant properties and molecular modeling studies of 2-amino-8*a*-methoxy-4*H*-pyrano[3,2-*c*]pyridine-3-carbonitriles, Eur. J. Med. Chem. 46 (2011) 2397−2407.

[38] F.M. Awadallah, W.I. El-Eraky, D.O. Saleh, Synthesis, vasorelaxant activity, and molecular modeling study of some new phthalazine derivatives, Eur. J. Med. Chem. 52 (2012) 14–21.

[39] Z.M. Nofal, A.M. Srour, W.I. El-Eraky, D.O. Saleh, A.S. Girgis, Rational design, synthesis and QSAR study of vasorelaxant active 3-pyridinecarbonitriles incorporating 1*H*-benzimidazol-2-yl function, Eur. J. Med. Chem. 63 (2013) 14−21.

[40] P.V. Oliferenko, A.A. Oliferenko, A.S. Girgis, D.O. Saleh, A.M. Srour, R.F. George, G.G. Pillai, C.S. Panda, C.D. Hall, A.R. Katritzky; Synthesis, bioassay, and molecular field topology analysis of diverse vasodilatory heterocycles, J. Chem. Inf. Model. 54 (2014**)** 1103–1116.

[41] A.S. Girgis, A.F. Mabied, J. Stawinski, L. Hegazy, R.F. George, H. Farag, E.M. Shalaby, I.S. Ahmed Farag, Synthesis and DFT studies of an antitumor active spiro-oxindole, N. J. Chem. 39 (2015) 8017−8027.

[42] A.F. Mabied, A.S. Girgis, E.M. Shalaby, R.F. George, B.E.M. El-Gendy, F.N. Baselious, Stereoselective synthesis, X-ray structure, spectroscopic characterization and geometry optimization of 4,5,11-triazatricyclo[6.2.1.0*2,6*]undec-5-ene , J. Heterocyclic Chem. (in press).

[43] M.A. Ibrahim, S.S. Panda, A.A. Oliferenko, P.V. Oliferenko, A.S. Girgis, M. Elagawany, F.Z. Küçükbay, C.S. Panda, G.G. Pillai, A. Samir, K. Tämm, C.D. Hall, A.R. Katritzky, Macrocyclic peptidomimetics with antimicrobial activity: synthesis, bioassay, and molecular modeling studies, Org. Biomol. Chem. 13 (2015) 9492–9503.

[44] S.S. Panda, S. Liaqat, A.S. Girgis, A. Samir, C.D. Hall, A.R. Katritzky, Novel antibacterial active quinolone–fluoroquinolone conjugates and 2D-QSAR studies**,** Bioorg. Med. Chem. Lett. 25 (2015) 3816–3821.

[45] R.N. Naumov, S.S. Panda, A.S. Girgis, R.F. George, M. Farhat, A.R. Katritzky, Synthesis and QSAR study of novel anti-inflammatory active mesalazine–metronidazole conjugates, Bioorg. Med. Chem. Lett. 25 (2015) 2314–2320.

[46] A.S. Girgis, S.S. Panda, M.N. Aziz, P.J. Steel, C.D. Hall, A.R. Katritzky, Rational design, synthesis, and 2D-QSAR study of anti-oncological alkaloids against hepatoma and cervical carcinoma, RSC Advances 5 (2015) 28554–28569.

[47] A.S. Girgis, S.S. Panda, E.M. Shalaby, A.F. Mabied, P.J. Steel, C.D. Hall, A.R. Katritzky, Regioselective synthesis and theoretical studies of an anti-neoplastic fluoro-substituted dispiro-oxindole, RSC Advances 5 (2015) 14780–14787.

[48] A.D. Tiwari, S.S. Panda, A.S. Girgis, S. Sahu, R.F. George, A.M. Srour, B. La Starza, A.M. Asiri, C.D. Hall, A.R. Katritzky, Microwave assisted synthesis and QSAR study of novel NSAID acetaminophen conjugates with amino acid linkers, Org. Biomol. Chem. 12 (2014) 7238–7249.

[49] E.M. Shalaby, A.S. Girgis, A.M. Moustafa, A.M. ElShaabiny, B.E.M. El-Gendy, A.F. Mabied, I.S. Ahmed Farag, Regioselective synthesis, stereochemical structure, spectroscopic characterization and geometry optimization of dispiro[3*H*-indole-3,2′-pyrrolidine-3′,3″-piperidines], J. Mol. Structure 1075 (2014) 327–334.

[50] R.F. George, N.S.M. Ismail, J. Stawinski, A.S. Girgis, Design, synthesis and QSAR studies of dispiroindole derivatives as new antiproliferative agents, Eur. J. Med. Chem. 68 (2013) 339–351.

[51] CODESSA-Pro manual p. 43, 67, 62.

[52] A.S. Girgis, D.O. Saleh, R.F. George, A.M. Srour, G.G. Pillai, C.S. Panda, A.R. Katritzky, Synthesis, bioassay, and QSAR study of bronchodilatory active 4*H*-pyrano[3,2-*c*]pyridine-3-carbonitriles, Eur. J. Med. Chem. 89 (2015) 835–843.

[53] http://michem.disat.unimib.it/chm/download/materiale/geometrical_descriptors.pdf.

[54] N.A. Shams, A.M. Kaddah, A.H. Moustafa, Reactions of 3-hydrazino-6-phenylpyridazines, Indian J. Chem., Sec.B, 21 (1982) 317–320.

[55] H. Jahine, H.A. Zaher, Y. Akhnookh, Z. El-Gendy, Reactions of 6-(*p*-chlorophenyl)-3-hydrazinopyridazine & 6-(*p*-chlorophenyl)pyridazine-3(2*H*)-thione, Indian J. Chem., Sec.B, 16 (11) (1978) 1000–1003.

[56] A.H. Shamroukh, A.E. Rashad, H.S. Ali, F.M.E. Abdel-Megeid, Some new pyrazole and pyrazolopyrimidines: Synthesis and antimicrobial evaluation, J. Heterocyclic Chem. 50 (2013) 758–765.

[57] A.H. Shamroukh, A.E. Rashad, H.S. Ali, S.M. Awad, Studies on the reactivity of amino-1-(6-phenyl-pyridazin-3-yl)-1*H*-pyrazole-4-carboxylic acid hydrazide towards some reagents for biological evaluation, J. Heterocyclic Chem. 51 (2014) 899–905.

Figure captions

Figure 1. Representative pyridazine based compounds with vasorelaxant activity.

Figure 2. General structures of the designed target compounds**.**

Figure 3. BMLR-QSAR plot of correlation representing the observed *vs.* predicted $1/IC_{50}$ (μM).

Table captions:

Table 1. Observed and predicted vasorelaxant activity (IC_{50}, μM) of the training set compounds **5a–d**, **6a–d**, **7a,c**, **8a–d**, **9a–d**, **10a–c**, **11a–c** and **12a–h** and doxazosin mesylate.

Table 2. Descriptor of the BMLR-QSAR model for the vasodilatory active pyridazines.

Table 3. Molecular descriptor values of the BMLR-QSAR model for the vasodilatory active pyridazines.

Table 4. Observed, predicated and molecular descriptor values of external test set compounds **7b** and **10d** according to the BMLR-QSAR model.

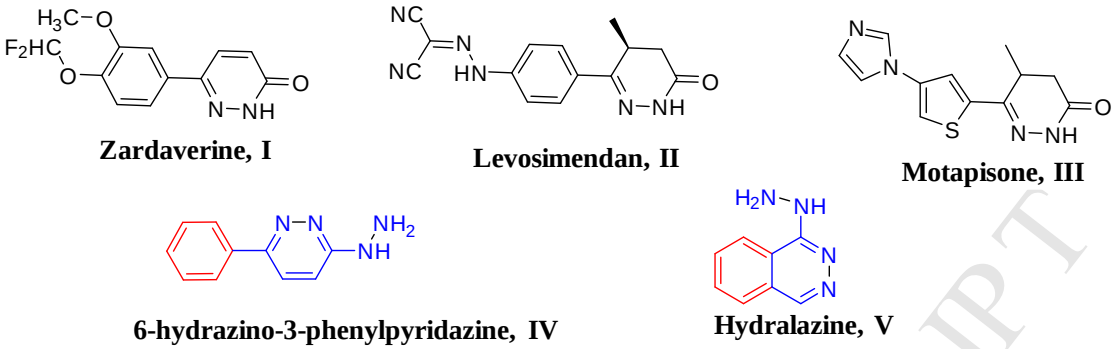

Figure 1. Representative pyridazine based compounds with vasorelaxant activity.

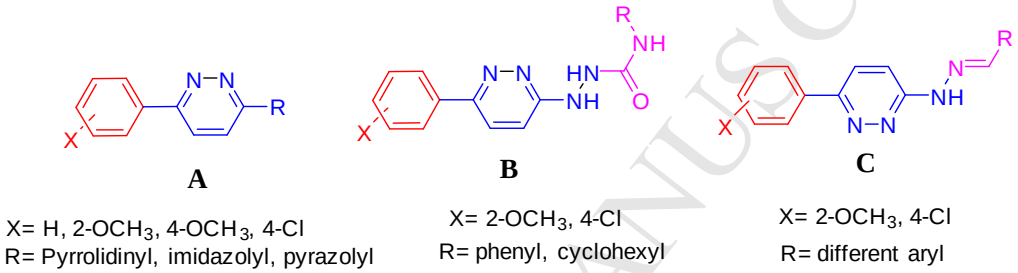

Figure 2. General structures of the designed target compounds**.**

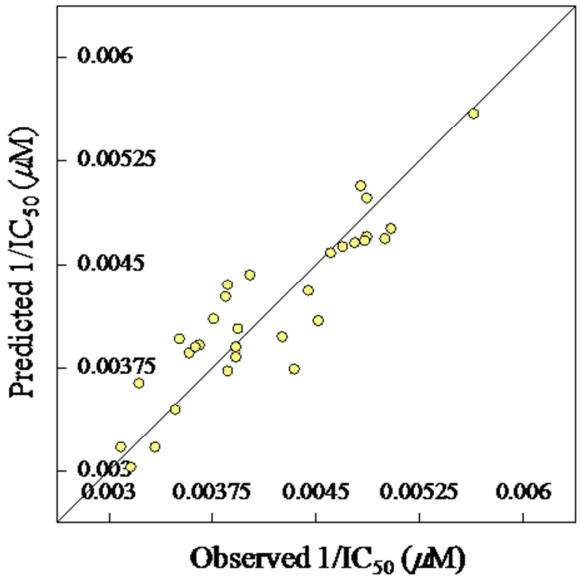

Figure 3. BMLR-QSAR plot of correlation representing the observed *vs.* predicted $1/IC_{50}$ (μM).

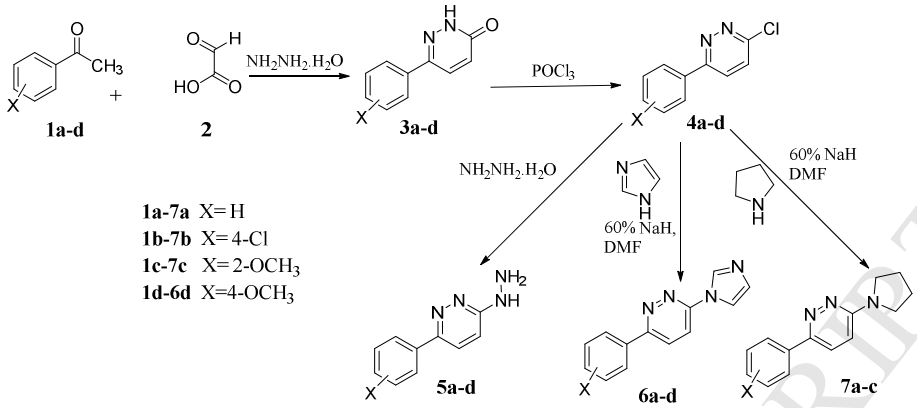

Scheme 1. Preparation of **6a-d** and **7a-c.**

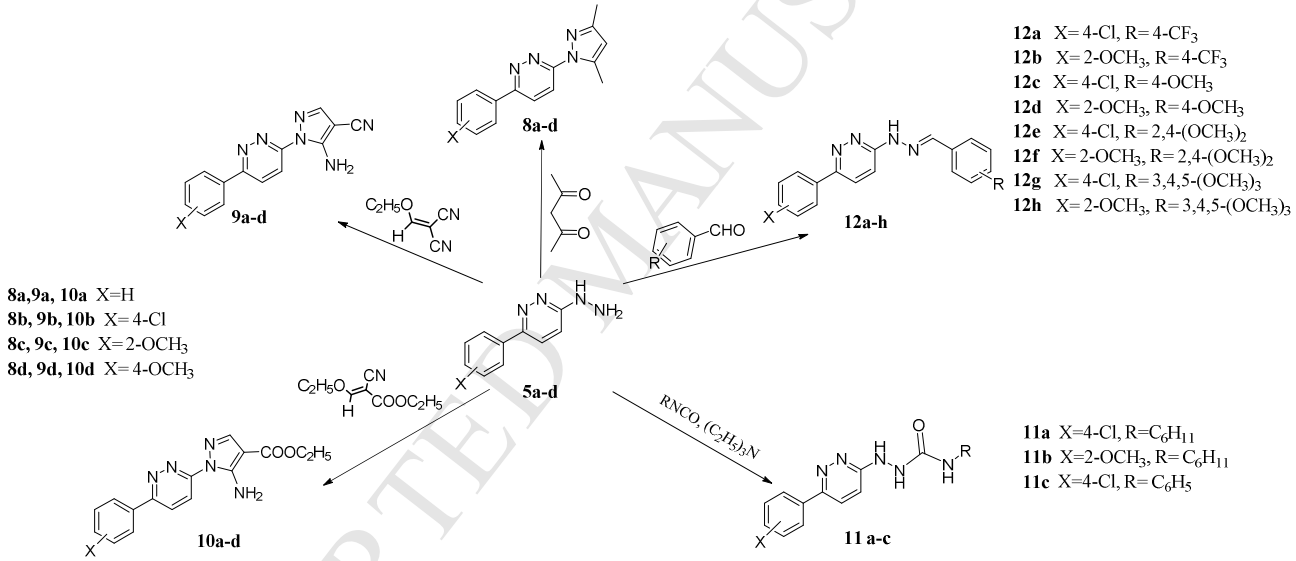

Scheme 2. Prepation of **8a-d, 9a-d, 10a-d, 11a-c** and **12a-h.**

Highlights

- Some phenylpyridazines were prepared by facile methods.
- They were screened for their vasorelaxant activity.
- Compounds 8a and 11a revealed promising activity compared to doxazosin mesylate.
- A reliable 2D-QSAR model was obtained to validate the obtained results.